PHYSICAL REVIEW B **80**, 241305(R) (2009)

Electron density dependence of the spin Hall effect in GaAs probed by scanning Kerr rotation microscopy

S. Matsuzaka,[1,2] Y. Ohno,[1,*] and H. Ohno[1,2,†]

[1]*Laboratory for Nanoelectronics and Spintronics, Research Institute of Electrical Communication, Tohoku University, Katahira 2-1-1, Aoba-ku, Sendai 980-8577, Japan*

[2]*ERATO Semiconductor Spintronics Project, Japan Science and Technology Agency, Tokyo, Japan*

(Received 3 August 2009; published 9 December 2009)

We studied electron density (n) dependence of the extrinsic spin Hall effect in n-doped GaAs with n raging from 1.8×10^{16} to 3.3×10^{17} cm^{-3}. By scanning Kerr microscopy measurements, we observed spin accumulation near the channel edges in all the samples due to the extrinsic spin Hall effect. The spin Hall conductivity σ^{SH} is obtained for each sample by comparing the Kerr rotation induced by optically injected spins. σ^{SH} is found to increase with n, and it is shown that a theoretical model reported earlier agrees well with the experimental n dependence of σ^{SH}.

DOI: 10.1103/PhysRevB.80.241305 PACS number(s): 72.25.Dc, 72.25.Pn, 85.75.−d

Observations of the spin Hall effect (SHE) (Refs. 1 and 2) and the current-induced spin polarization[3–5] in semiconductors have been reported in the route of exploring a possibility for electrical generation and manipulation of spin currents. In particular, SHE has attracted much attention since pure spin current can be generated in nonmagnetic material without using ferromagnetic material or applying an external magnetic field. In the SHE, an electrical current induces transverse pure spin current in nonmagnetic material resulting in spin accumulation at sample boundaries without charge accumulation. Similar to the anomalous Hall effect, spin-orbit interaction is the origin of the SHE, which can be classified into the "extrinsic" SHE,[6,7] which is induced by impurity scattering, and the "intrinsic" SHE,[8,9] which results from the band-structure Berry phase acquired by the moving charge. Kato *et al.* first reported experimental observation of local spin accumulation at the sample edges in n-GaAs and n-InGaAs.[1] Subsequently, Wunderlich *et al.* showed circularly polarized light emission in a pn-junction-based structure due to spin-polarized holes at the edges of the structure.[2] The former has been explained in terms of the extrinsic SHE because the spin Hall conductivity σ^{SH} is small and independent of crystal orientation, while the latter has been attributed to the intrinsic SHE.

The extrinsic SHE in doped semiconductors has been further studied in quantum well structures,[10] different materials,[11] and specific sample geometry to elucidate the nature of the SHE.[12,13] Moreover, time-resolved dynamics of spin accumulation induced by SHE has been demonstrated.[14] Theoretical studies have also been put forward to explain the origin of the SHE (Refs. 15 and 16) revealing how the extrinsic SHE should depend on the basic semiconductor parameters such as the doping density. In the following, we investigate the electron density (n) dependence of SHE in n-doped GaAs. We determine σ^{SH} as a function of n ranging from 1.8×10^{16} to 3.3×10^{17} cm^{-3} by comparing the local spin accumulation induced by SHE with the optically injected spins in n-GaAs. The results are compared with a theory put forward earlier.

In this study, five samples (labeled by A–E) with different doping concentrations on undoped (100) GaAs substrate grown by molecular beam epitaxy are used. They consist of a 2-μm-thick Si-doped GaAs grown on a 400 nm $Al_{0.3}Ga_{0.7}As$ barrier and an undoped GaAs buffer layer. All samples have a 250-μm-long and 60-μm-wide Hall-bar structure with alloyed Ohmic contacts of Au/Ni/AuGe/Ni. The conductivity σ^c and the electron density n (cm^{-3}) are obtained by the Hall measurement done at 30 K with applying an electric field E of 5 mV/μm. Taking into account the surface depletion, σ^c, n, and the effective thickness d_{eff} of n-GaAs are calculated. The electron g factor g and spin relaxation time τ_s^{OP} are evaluated from the results of time-resolved Kerr rotation measurements at low external magnetic field (<0.5 T). τ_s^{OP} longer than the pulse interval (samples A–C) is determined by using a resonant spin amplification technique.[17] These data are summarized in Table I.

In order to probe the local spin polarizations induced by the SHE and by the optical spin injection, we implemented a spatially resolved scanning Kerr microscopy (SKM) system as shown in Fig. 1. As a source of the probe light, we employed a mode-locked Ti:sapphire laser, which generates 3 ps (the linewidth is less than 1 meV) pulse trains at 76 MHz repetition rate. The probe light intensity is 110 μW, and the photon energy is fixed at 1.503 eV, which is lower than the band gap of n-GaAs, in order to avoid optical excitation of excess electron-hole pairs in the sample. The Hall-bar sample is placed in a He-flow cryostat with an optical window and kept at 30 K. In SKM measurements, we take the origin of the coordinate at the center of the Hall bar, and the

TABLE I. Physical properties of samples A–E studied in this work.

Sample	σ^c (Ω^{-1} m^{-1})	n (cm^{-3})	d_{eff} (μm)	g	τ_s^{OP} (ns)	R
A	3200	1.8×10^{16}	1.76	0.438	38.2	0.30
B	3500	2.9×10^{16}	1.81	0.423	22.4	0.31
C	4400	5.1×10^{16}	1.86	0.407	12.6	0.30
D	9400	1.4×10^{17}	1.91	0.356	2.53	0.31
E	16000	3.3×10^{17}	1.94	0.284	1.06	0.34

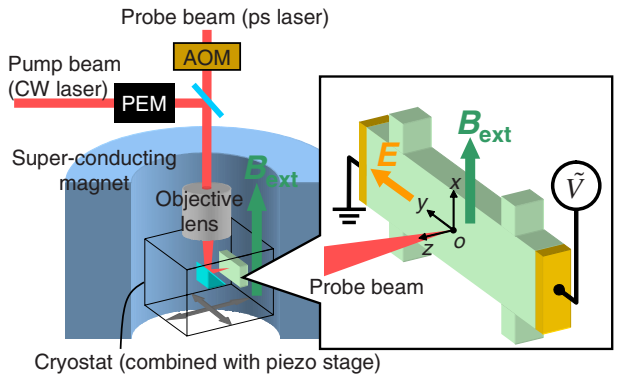

FIG. 1. (Color online) A schematic illustration of the scanning Kerr microscopy system and the sample configuration.

x and y axes are taken to be across and along the Hall-bar channel, respectively. An external magnetic field B_{ext} is applied in the x direction. The path of the probe light, whose intensity is modulated by acousto-optical modulator at f_a=50.6 kHz, is bent 90° by a prism mirror placed in the cryostat to detect the out-of-plane (z) component of spins in the sample by measuring the Kerr rotation angle. The spot size on the sample was $\omega_0 \sim 1.25$ μm, where ω_0 is Gaussian beam radius. An SKM image is taken by moving the cryostat integrated on a piezo nanoscanning stage. In SHE measurements, an ac electric field E is applied along the y direction at the frequency of 1 kHz. The Kerr rotation angle of the probe beam induced by the SHE, labeled by θ_K^{SH}, is then measured by using a balanced photoreceiver and a lock-in amplifier at 1 kHz. For the measurements of optically injected spins, we use a cw Ti:sapphire laser as a pump light source. The helicity of the pump light is modulated by photoelastic modulator at f_p=50.1 kHz. The pump beam is led onto the same path of the probe light via beam splitter and focused on the same position with the same spot size of the probe light. The power of the pump light I_{pump} is set to be 8–23 μW and the photon energy E_{pump} was set well above the absorption edges of the samples; 1.521 eV for samples A–D and 1.531 eV for sample E. The Kerr rotation due to the photoexcited electron spins, labeled by θ_K^{OP}, is detected by a balanced photoreceiver and a lock-in amplifier tuned at $f_a - f_p$=0.5 kHz. The reflectivity R of each sample at E_{pump} is evaluated by reflection measurements (shown in Table I).

First we examine the n dependence of the SHE. Spatial profiles of the Kerr rotation $\theta_K^{SH}(x)$ across the channel measured at y=0 and E=5 mV/μm are shown by open symbols in Fig. 2(a). In all the samples, peak structures near the channel edges are clearly shown. Figure 2(b) shows the Hanle curves by open symbols as a function of B_{ext}, which were measured at the peak position of $\theta_K^{SH}(x)$. These features are consistent with the results reported in Ref. 1. Based on the drift-diffusion model,[1,8,18] the z component of the spin density per unit volume, $S_z^{SH}(x)$, is given by $(E\sigma^{SH}\tau_s^{SH}/L_s^{SH})\sinh(x/L_s^{SH})/\cosh(L_{eff}/2L_s^{SH})$, where L_s^{SH} is the spin diffusion length and τ_s^{SH} is the spin relaxation time under the application of E. L_{eff} is the distance between the peaks of $\theta_K^{SH}(x)$ on both edges. In our SKM system, the probe beam profile has a symmetric Gaussian shape and is expressed as $\exp\{-2(X^2+Y^2)/\omega_0^2\}$. Assuming that $\theta_K^{SH}(x)$ is

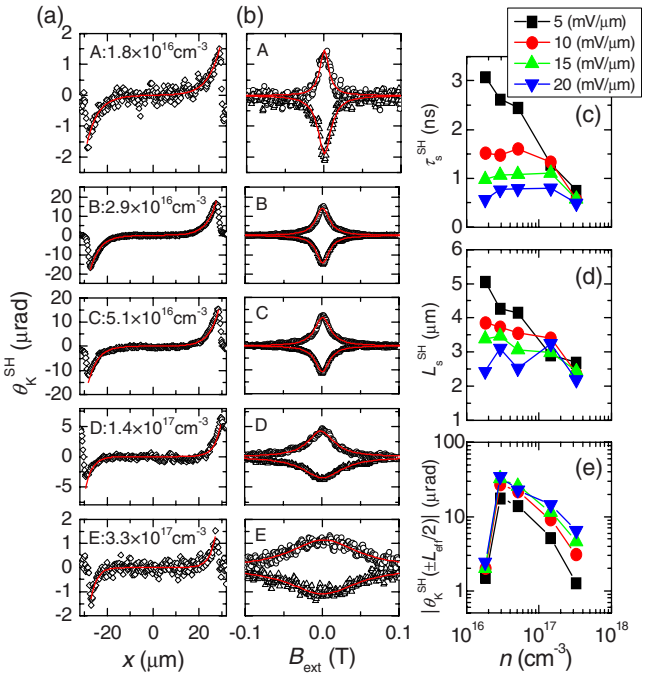

FIG. 2. (Color online) (a) Spatial profiles of $\theta_K^{SH}(x)$ across the channel and (b) Hanle curves of $\theta_K^{SH}(x=\pm L_{eff}/2)$ as a function of B_{ext} measured at y=0 and E=5 mV/μm. Open symbols are experimental data and (red) lines are fitting results. Constant offsets have been subtracted. (c)–(e) E dependence of τ_s^{SH}, L_s^{SH}, and $|\theta_K^{SH}(\pm L_{eff}/2)|$ for all the samples as a function of n determined at E=5–20 mV/μm.

proportional to total amount of z component of the spins with a constant C_0^{SH}, then

$$\theta_K^{SH}(x) = d_{eff}C_0^{SH}\int\int_S \exp[-2(X^2+Y^2)/\omega_0^2]S_z^{SH}(X-x)dS$$

$$= (d_{eff}C_0^{SH}E\sigma^{SH}\tau_s^{SH}/L_s^{SH})\sqrt{2\pi}\omega_0 C^{SH}(x)/2, \quad (1)$$

where $C^{SH}(x) = \int_{-\infty}^{+\infty}\exp(-2X^2/\omega_0^2)\sinh[(X-x)/L_s^{SH}]/\cosh(L_{eff}/2L_s^{SH})dX$. The experimental data shown in Fig. 2(a) can be fitted well by Eq. (1) as indicated by a (red) line, from which L_s^{SH} and the peak values of $\theta_K^{SH}(x)$ at $x=\pm L_{eff}/2$ are obtained. In Fig. 2(b), the Hanle curve obtained at the boundary for each sample is fitted by a Lorentz function $\theta_K^{SH}(\pm L_{eff}/2)/\{1+(g\mu_B B_{ext}\tau_s^{SH}/\hbar)^2\}$, as shown by a (red) line.[13] Here, μ_B is the Bohr magneton and $\hbar$ is the reduced Planck constant. From the fitting, τ_s^{SH} is obtained. For all the samples with different n's, E dependence (5–20 mV/μm) of τ_s^{SH}, L_s^{SH}, and $|\theta_K^{SH}(\pm L_{eff}/2)|$ are shown in Figs. 2(c)–2(e) as a function of n. The decrease in τ_s^{SH} and L_s^{SH} with increasing n reflects the enhanced spin relaxation due to the D'yakonov-Perel' mechanism.[19] When E is increased, τ_s^{SH} and L_s^{SH} decrease again by the D'yakonov-Perel' mechanism as a result of the increase in the electron temperature.[20] As shown in Fig. 2(e), $|\theta_K^{SH}(\pm L_{eff}/2)|$ increases with E and tends to saturate, as observed in Ref. 1. It should be noted in Fig. 2(e) that $|\theta_K^{SH}(\pm L_{eff}/2)|$ does not change with n monotonically. This reflects the fact that C_0^{SH} is sample dependent, and

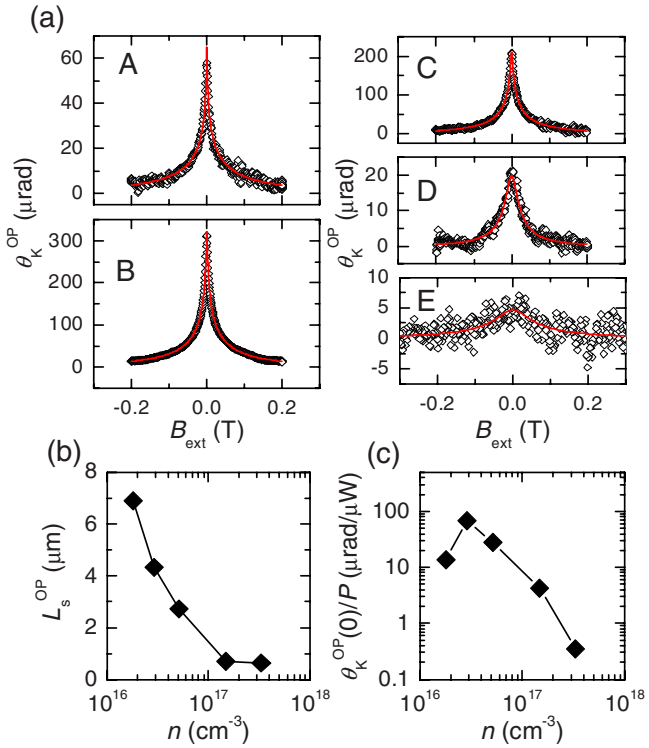

FIG. 3. (Color online) (a) Hanle curves of θ_K^{OP} as a function B_{ext}. Open symbols are experimental data and (red) lines are fitting results to the data. Constant offsets have been subtracted. (b) L_s^{OP} and $\theta_K^{OP}(0)/P$ determined by optical spin injection measurements as a function of n.

thus the calibration between the Kerr rotation angle and S_z is necessary.

In order to establish the relation between the Kerr rotation angle and S_z for each sample, we optically inject spins and measure the Kerr rotation by using the SKM system at the origin of the samples. In Fig. 3(a), experimental results of $\theta_K^{OP}(B_{ext})$ are shown as a function B_{ext}. To derive the relation between $\theta_K^{OP}(B_{ext})$ and the spatial distribution of the z component of optically injected spin per unit area, $S_z^{OP}(r)$, we employed a model described in Ref. 21. Taking into account that the spin polarization of optically injected electrons is 50% due to the optical selection rule,

$$S_z^{OP}(r) = \frac{\tau_s^{OP}}{2\pi(L_s^{OP})^2}\frac{P}{2E_{pump}}\mathrm{Re}\left[K_0\left(\frac{r}{L_s^{OP}}\sqrt{1+i\Omega\tau_s^{OP}}\right)\right], \tag{2}$$

where $\Omega = g\mu_B B_{ext}/\hbar$ is the Larmor precession frequency, r is the distance from the center of the pump light spots, L_s^{OP} is the spin diffusion length of optically injected spins (at $E=0$), E_{pump} is the photon energy of the pump light, and K_0 is the zero-order modified Bessel function of the second kind. P is the amount of the absorbed light intensity in n-GaAs: in this work, we use $P = I_{pump}(1-R)\{1-\exp(-d\alpha)\}$, where d is the thickness of n-GaAs (2 μm) and α is taken to be 10^4 cm^{-1} for all the samples.[22] Then, $\theta_K^{OP}(B_{ext})$ induced by $S_z^{OP}(r)$ is given by

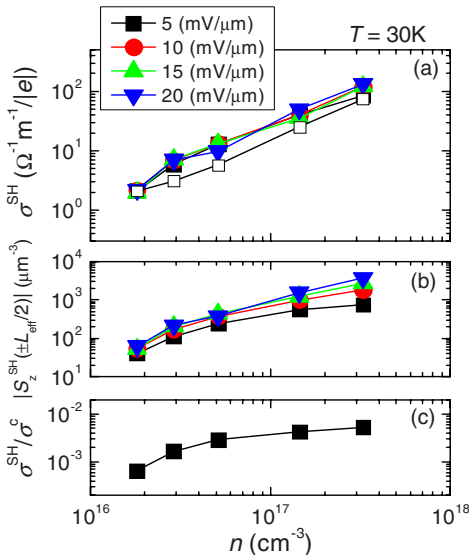

FIG. 4. (Color online) (a)–(c) E dependence of σ^{SH}, $|S_z^{SH}(\pm L_{eff}/2)|$, and σ^{SH}/σ^c as a function of n. Solid symbols show experimentally determined value and open symbols show calculated σ^{SH} for $E=5$ mV/μm.

$$\theta_K^{OP}(B_{ext}) = C_0^{OP}\int\int_S \exp(-2r^2/\omega_0^2)S_z^{OP}(r)dS$$
$$= \frac{C_0^{OP}\tau_s^{OP}}{(L_s^{OP})^2}\frac{P}{2E_{pump}}C^{OP}(B_{ext}), \tag{3}$$

where

$$C^{OP}(B_{ext}) = \int_0^{+\infty} r\exp(-2r^2/\omega_0^2) \times \mathrm{Re}[K_0((r/L_s^{OP})\sqrt{1+i\Omega\tau_s^{OP}})]dr.$$

Using Eq. (3), we fit the data shown in Fig. 3(a) with C_0^{OP} and L_s^{OP} as fitting parameters. As indicated by (red) lines, the fit reproduces the data well, from which L_s^{OP} is obtained. In Fig. 3(b) and 3(c), n dependence of L_s^{OP} and $\theta_K^{OP}(0)/P$ are shown. L_s^{OP} decreases with increasing n, similarly to the result of L_s^{SH} under applied electric fields. In Fig. 3(c), $\theta_K^{OP}(0)/P$ shows nonmonotonic n dependence, like in the case of $|\theta_K^{SH}(\pm L_{eff}/2)|$ [see Fig. 2(e)], reflecting the sample dependence of C_0^{OP}.

Since the photon energy of the probe light is the same for both SHE and optical spin injection experiments, it is reasonable to take $C_0^{SH} = C_0^{OP}$ for each sample. Based on this, we calculate σ^{SH} from Eqs. (1) and (3) using the experimentally obtained values $|\theta_K^{SH}(\pm L_{eff}/2)|$ and $\theta_K^{OP}(0)$. In Figs. 4(a)–4(c), σ^{SH}, $|S_z^{SH}(\pm L_{eff}/2)|$, and σ^{SH}/σ^c are indicated by solid symbols as functions of n. It is shown in Fig. 4(a) that σ^{SH} increases with n and is almost independent of E.[1]

Finally, we refer to the theoretical expression of σ^{SH},[16] which is given by

$$\sigma^{SH} = \left|\frac{-\pi m\lambda_0^2\varepsilon_F\sigma^c}{3\hbar^2} + \frac{e^2\lambda_0^2}{4\hbar}n\right|, \tag{4}$$

where m is the effective mass of electron, e is the elementary charge, and ε_F is the Fermi energy referred to as

$\varepsilon_F = 5.209 \times 10^{-14} n^{2/3} - 1.456 \times 10^{-27} n^{4/3}$ eV at low temperature.[23] The calculated σ^{SH} by using Eq. (4) are shown by open symbols in Fig. 4(a). In the calculation, we used n and σ^c in Table I and $\lambda_0 = 4.7 \times 10^{-8}$ cm.[16] σ^{SH} derived from Eq. (4) reproduces well the experimental σ^{SH}. As n increases, $|S_z^{SH}(\pm L_{eff}/2)|$ tends to saturate up to the corresponding spin polarization of around 1%. This indicates that the spin accumulation is reduced by enhanced spin relaxation due to the D'yakonov-Perel' mechanism, while the spin current induced by SHE is enhanced by increasing n. It is found that the order of the spin Hall angle σ^{SH}/σ^c is $10^{-2}-10^{-3}$ and tends to increase with n but saturates when n is increased to 10^{17} cm^{-3}.

In conclusion, we have studied electron density dependence of the extrinsic SHE and spin Hall conductivity in n-doped GaAs by scanning Kerr microscopy. We have observed the Kerr rotation signal due to the spin accumulation near the channel edges in n-GaAs with n raging from 1.8×10^{16} to 3.3×10^{17} cm^{-3}. Based on a quantitative analysis of optical spin injection and SKM detection, we show that σ^{SH} is enhanced by increasing n, and σ^{SH}/σ^c saturates at 10^{-2}. We have also shown that the theoretical model proposed in Ref. 16 well explains our experimental data.

We thank K. Ohtani and F. Matsukura for discussions. This work was partly supported by ERATO, JST, the Grant-in-Aid for Scientific Research (Contracts No. 19048007 and No. 19048008 in Priority Area "Creation and control of spin current") from the Ministry of Education, Culture, Sports, Science and Technology (MEXT).

*oono@riec.tohoku.ac.jp
†ohno@riec.tohoku.ac.jp

[1] Y. K. Kato, R. C. Myers, A. C. Gossard, and D. D. Awschalom, Science **306**, 1910 (2004).
[2] J. Wunderlich, B. Kaestner, J. Sinova, and T. Jungwirth, Phys. Rev. Lett. **94**, 047204 (2005).
[3] L. E. Vorob'ev, E. L. Ivchenko, G. E. Pikus, I. I. Farbshtein, V. A. Shalygin, and A. V. Shturbin, JETP Lett. **29**, 441 (1979).
[4] Y. K. Kato, R. C. Myers, A. C. Gossard, and D. D. Awschalom, Phys. Rev. Lett. **93**, 176601 (2004).
[5] A. Yu. Silov, P. A. Blajnov, J. H. Wolter, R. Hey, K. H. Ploog, and N. S. Averkiev, Appl. Phys. Lett. **85**, 5929 (2004).
[6] M. I. D'yakonov and V. I. Perel', JETP Lett. **13**, 467 (1971).
[7] J. E. Hirsch, Phys. Rev. Lett. **83**, 1834 (1999).
[8] S. Murakami, N. Nagaosa, and S. C. Zhang, Science **301**, 1348 (2003).
[9] J. Sinova, D. Culcer, Q. Niu, N. A. Sinitsyn, T. Jungwirth, and A. H. MacDonald, Phys. Rev. Lett. **92**, 126603 (2004).
[10] V. Sih, R. C. Myers, Y. K. Kato, W. H. Lau, A. C. Gossard, and D. D. Awschalom, Nat. Phys. **1**, 31 (2005).
[11] N. P. Stern, S. Ghosh, G. Xiang, M. Zhu, N. Samarth, and D. D. Awschalom, Phys. Rev. Lett. **97**, 126603 (2006).
[12] V. Sih, W. H. Lau, R. C. Myers, V. R. Horowitz, A. C. Gossard, and D. D. Awschalom, Phys. Rev. Lett. **97**, 096605 (2006).
[13] N. P. Stern, D. W. Steuerman, S. Mack, A. C. Gossard, and D. D. Awschalom, Appl. Phys. Lett. **91**, 062109 (2007).
[14] N. P. Stern, D. W. Steuerman, S. Mack, A. C. Gossard, and D. D. Awschalom, Nat. Phys. **4**, 843 (2008).
[15] H.-A. Engel, B. I. Halperin, and E. I. Rashba, Phys. Rev. Lett. **95**, 166605 (2005).
[16] W.-K. Tse and S. Das Sarma, Phys. Rev. Lett. **96**, 056601 (2006).
[17] J. M. Kikkawa and D. D. Awschalom, Phys. Rev. Lett. **80**, 4313 (1998).
[18] S. Zhang, Phys. Rev. Lett. **85**, 393 (2000).
[19] R. I. Dzhioev, K. V. Kavokin, V. L. Korenev, M. V. Lazarev, B. Ya. Meltser, M. N. Stepanova, B. P. Zakharchenya, D. Gammon, and D. S. Katzer, Phys. Rev. B **66**, 245204 (2002).
[20] M. Beck, C. Metzner, S. Malzer, and G. H. Dohler, EPL **75**, 597 (2006).
[21] M. Furis, D. L. Smith, S. Kos, E. S. Garlid, K. S. M. Reddy, C. J. Palmstrom, P. A. Crowell, and S. A. Crooker, New J. Phys. **9**, 347 (2007).
[22] C. J. Hwang, J. Appl. Phys. **40**, 3731 (1969).
[23] N.-Y. Lee, K.-J. Lee, C. Lee, J.-E. Kim, H. Y. Park, D.-H. Kwak, H.-C. Lee, and H. Lim, J. Appl. Phys. **78**, 3367 (1995).